11th International Symposium on Turbulence and Shear Flow Phenomena (TSFP11)
Southampton, UK, July 30 to August 2, 2019

DIRECT NUMERICAL SIMULATION OF TEMPORALLY DEVELOPING GRID TURBULENCE

Tomoaki Watanabe
Department of Aerospace Engineering
Nagoya University
Nagoya 464-8603, Japan
watanabe.tomoaki@c.nagoya-u.jp

Koji Nagata
Department of Aerospace Engineering
Nagoya University
Nagoya 464-8603, Japan
nagata@nagoya-u.jp

ABSTRACT

Direct numerical simulations (DNSs) of temporally developing grid turbulence at mesh Reynolds numbers of $Re_M = 10,000$ and $20,000$ are performed in a periodic box. The simulations are initialized with a velocity field that approximates the wakes induced by the bars of conventional square grids. The turbulence statistics obtained in the temporal DNS agree well with those of the previous experiments. The decay exponents n of the turbulent kinetic energy are close to the values for Saffman turbulence.

INTRODUCTION

One of the simplest turbulent flows is homogeneous isotropic turbulence, for which a large number of turbulence theories and models have been developed. Without an external force, turbulent kinetic energy in homogeneous isotropic turbulence decays with time. In experiments, grid turbulence has been studied since the earlier experiments of Simmons & Salter (1934) to investigate the decay exponent of freely decaying, quasi homogeneous isotropic turbulence. It has been widely accepted that turbulent kinetic energy of grid turbulence follows the power law in the decay region far from the grid (typically $x \geq 40M$-$50M$). This decay law for the streamwise velocity variance (i.e., one component of the turbulent kinetic energy) can be written as

$$\frac{\langle u^2 \rangle}{U_0^2} = A\left(\frac{x}{M} - \frac{x_0}{M}\right)^{-n}, \tag{1}$$

where $\langle u^2 \rangle$ is the variance of streamwise velocity fluctuations; U_0 is the mean wind speed; M is the mesh size; x is the streamwise distance from the grid; x_0 is the virtual origin; A is the decay constant; n is the decay exponent. Recent experiments (e.g., Krogstad & Davidson, 2010; Kitamura *et al.*, 2014; Sinhuber *et al.*, 2015) have shown that n is close to Saffman's prediction of 6/5. On the other hand, the grid turbulence that follows Kolmogorov decay law in the final period of decay was also reported in the wind tunnel experiments (Batchelor & Townsend, 1948).

In this study, we perform direct numerical simulations (DNSs) of the grid turbulence in a periodic box based on the temporal approach. Temporal simulations have been performed for turbulent shear flows, such as jets, wakes, mixing layers, and boundary layers (e.g., Kozul *et al.*, 2016; Watanabe *et al.*, 2018) and have proven to be very effective for studying various canonical flows. These temporal simulations use the periodic boundary condition in the streamwise direction even if all these flows are inhomogeneous in this direction. Despite the success of the temporal simulations of canonical flows, grid turbulence has not been considered in this manner. The temporal DNS has a great advantage against the spatial DNS in terms of computational cost. A flow past a grid is inhomogeneous in transverse directions, and there exist a strong shear region, which leads to the formation of grid turbulence. We can also interpret the production of grid turbulence as the process by which turbulent wakes of a large number of bars merge until the mean velocity becomes homogeneous in the transverse direction. Turbulence statistics in temporally developing turbulence are compared with those in previous grid turbulence experiments. The decay exponents n are also calculated and discussed.

NUMERICAL METHODS

DNS is performed for grid turbulence generated by a square grid with a mesh size M (solidity is $\sigma = 0.36$) towed with speed U_0. The mesh Reynolds numbers are $Re_M = U_0 M/\nu = 10,000$ and $20,000$, where ν is the kinematic viscosity. We consider a cubic computational domain with a side length l, where the periodic boundary conditions are applied in three directions. The flow is initialized by a mean streamwise velocity that is equal to U_0 behind the bars and 0 behind the holes of the grid. Furthermore, following to previous studies of turbulent free shear flows, the homogeneous isotropic velocity fluctuation with rms velocity $0.05U_0$ is added to all components of velocity vector for triggering the turbulent transition of the wake of each bar. Figure 1 shows the initial streamwise velocity on the bound-

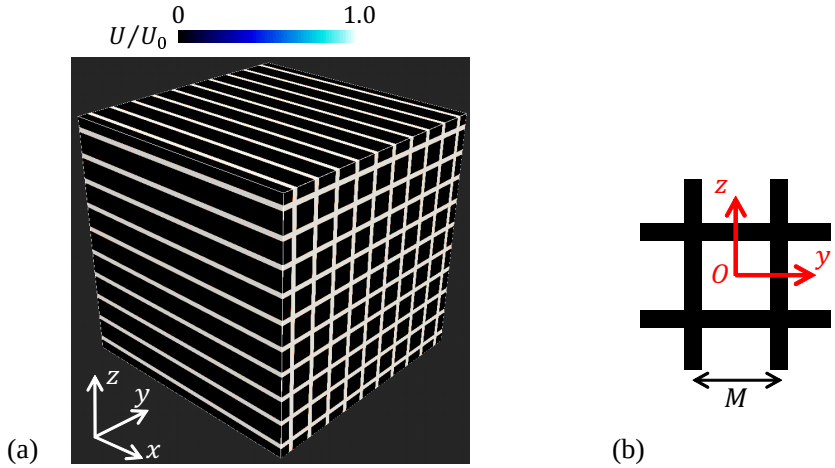

Figure 1. (a) Initial streamwise velocity on the boundaries of the computational box. (b) Statistics are computed in the coordinate whose origin is located at the center of the grid.

Table 1. Parameters in the DNS.

Run	Re_M	l	N^3
Re1	$10,000$	$20M$	$2,304^3$
Re2	$20,000$	$10M$	$2,048^3$

aries of the computational box. The computational domain is represented by N^3 grid points. Table 1 summarizes the parameters in the DNS.

The governing equations are incompressible Navier–Stokes equations. The DNS code is the same as used in Watanabe *et al.* (2018). The time is advanced from the initial field based on the fractional step method. The spatial derivative is computed by a fourth-order fully conservative finite difference, whilst time is advanced using the third-order Runge–Kutta method. The Poisson equation is solved using the Bi-CGSTAB method. In each time step, statistics are computed with spatial average $\langle\cdot\rangle$ as a function of (y,z) with the origin at the grid center as in Fig. 1(b). The length $X = tU_0$ in the temporally developing grid turbulence is equivalent to a streamwise distance x from the grid in spatially developing grid turbulence in wind tunnel experiments. Therefore, temporally developing grid turbulence is compared with spatially developing grid turbulence by plotting the results against x/M or $X/M = t/t_r$, where $t_r = M/U_0$. The DNSs are performed until $t = 1,024t_r$.

RESULTS ANS DISCUSSIONS

Figures 2 and 3 show the instantaneous streamwise velocity U on a y-z plane from $t/t_r = 2$ to 16 in the DNS at $Re_M = 10,000$. The imprint of the initial mean velocity profile clearly remains for an early time. The shear that results from the mean velocity causes the turbulent wakes of the bars to grow with time, as shown in Figs. 2. The turbulent wakes produced by the bar merge to form the grid turbulence in Figs. 3.

Figure 4 shows the temporal evolutions of mean streamwise velocity $\langle U\rangle_x$ and streamwise velocity variance $\langle u^2\rangle$ at three locations of (y,z), where $u = U - \langle U\rangle$ is the streamwise velocity fluctuation. The mean velocity becomes homogeneous at $t/t_r \approx 25$ and maintains a constant value $\langle U\rangle_x/U_0 = 0.36$ for the large t. This value is related to σ. Similarly, the velocity variance becomes independent of (y,z) with time. Figure 4(b) compares the temporally-developing grid turbulence with the grid turbulence realized in wind tunnels (Melina *et al.*, 2016; Nagata *et al.*, 2017) and the towed grid turbulence (Dickey & Mellor, 1980; Liu, 1995). The decay of $\langle u^2\rangle/U_0^2$ in the temporally-developing grid turbulence agrees well with those in previous experiments.

The decay exponent n is estimated by applying a nonlinear least-squares method (the Levenberg-Marquardt method) to the decay law $\langle u^2\rangle$. Once the grid turbulence decays and the turbulent Reynolds number becomes very small, the non-dimensional dissipation rate $C_\varepsilon = \langle\varepsilon\rangle L_u/\langle u^2\rangle^{3/2}$ also varies with time, where $\langle\varepsilon\rangle$ is the turbulent kinetic energy dissipation rate and L_u is the integral length scale obtained by the longitudinal auto-correlation function. Time dependence of the non-dimensional dissipation rate C_ε also affects n. For $Re_M = 20,000$, the fitting is applied for $100t_r \le t \le 500t_r$, for which C_ε does not vary with time. On the other hand, C_ε increases with time for $t \ge 100t_r$ in the decay region at $Re_M = 10,000$. The fitting is applied for $200t_r \le t \le 900t_r$ in the case of $Re_M = 10,000$. The decay exponents obtained in this way are $n = 1.22$ at $Re_M = 20,000$ and $n = 1.36$ at $Re_M = 10,000$. The former value at $Re_M = 20,000$ is fairly close to the decay exponent obtained for the Saffman turbulence $n = 6/5$. Wind tunnel experiments (e.g., Krogstad & Davidson, 2010; Kitamura *et al.*, 2014; Sinhuber *et al.*, 2015; Hearst & Lavoie, 2016) also reported the decay exponent close to $6/5$. For $Re_M = 10,000$, C_ε increases with time as $C_\varepsilon = C\,(t/(M/U_0) - t_0/(M/U_0))^{-p}$, where $t_0 = x_0/U_0$ is obtained from the decay of $\langle u^2\rangle$. The least square method applied to C_ε at $Re_M = 10,000$ yields $p = 0.13$. In this case, the Saffman turbulence has a modified decay exponent $n = 6(1+p)/5 = 1.35$ (Krogstad & Davidson, 2010), which is close to the value obtained from the decay of $\langle u^2\rangle$.

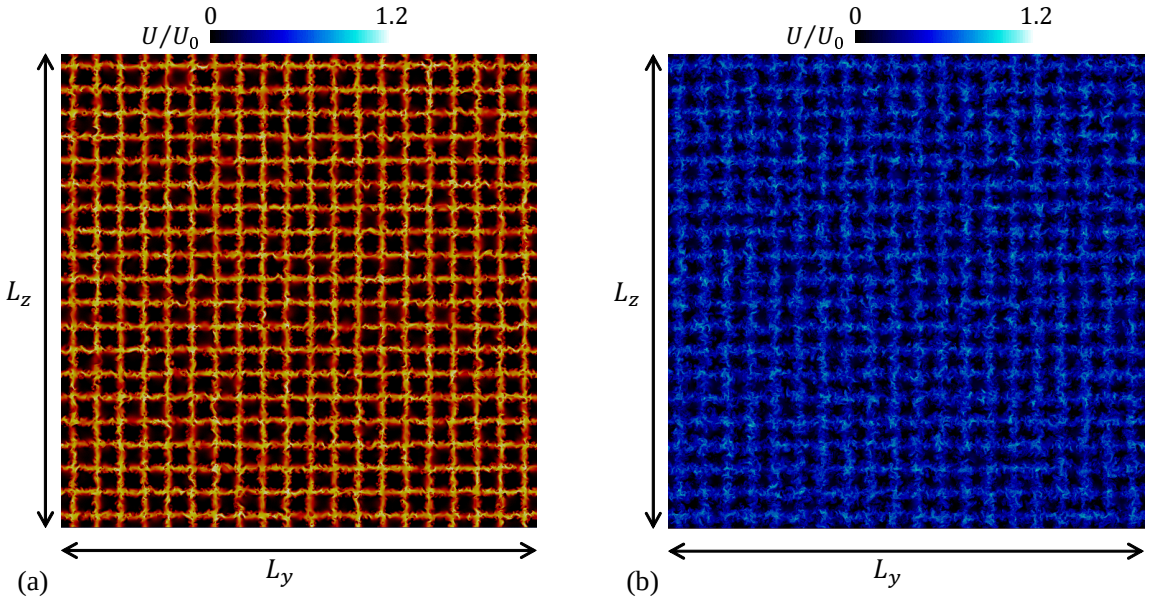

Figure 2. Instantaneous streamwise velocity U on a y-z plane at (a) $t/t_r = 2$ and (b) $t/t_r = 4$ for $Re_M = 10,000$.

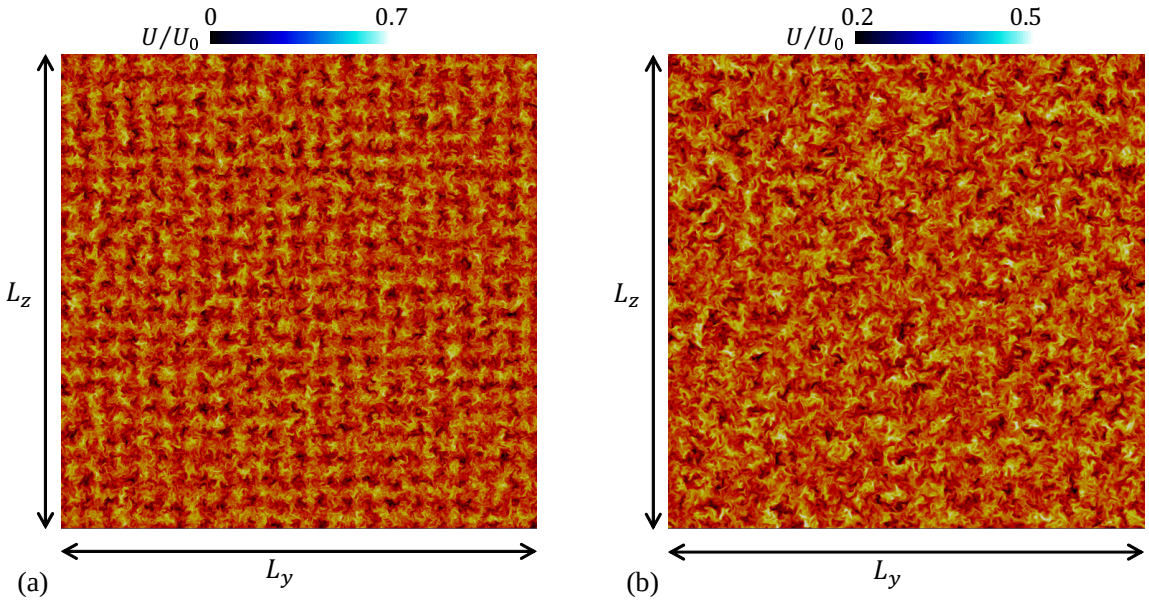

Figure 3. Instantaneous streamwise velocity U on a y-z plane at (a) $t/t_r = 8$ and (b) $t/t_r = 16$ for $Re_M = 10,000$.

SUMMARY

DNSs of temporally developing grid turbulence at mesh Reynolds numbers of $Re_M = 10,000$ and $20,000$ are performed in a periodic box and the statistics are shown to be in good agreements with the previous experiments. The decay exponents n of TKE are close to the values for Saffman turbulence. The DNS is initialized by a velocity profile that approximates the wakes of the bars even though this initial condition is much simpler than the actual grid turbulence. The present results imply that the transverse profile of the mean streamwise velocity plays important roles in formation of grid turbulence that follows the Saffman decay law.

Acknowledgements

The numerical simulations were carried out on the high-performance computing system (NEC SX-ACE) in the Japan Agency for Marine-Earth Science and Technology. This work was supported by JSPS KAKENHI Grant Numbers 18H01367 and 18K13682 and partially by the 'Collaborative Research Project on Computer Science with High-Performance Computing in Nagoya University.'

REFERENCES

Batchelor, G. K. & Townsend, A. A. 1948 Decay of isotropic turbulence in the initial period. *Proceedings of the Royal Society A* **193**, 539–558.

Dickey, T. D. & Mellor, G. L. 1980 Decaying turbulence in

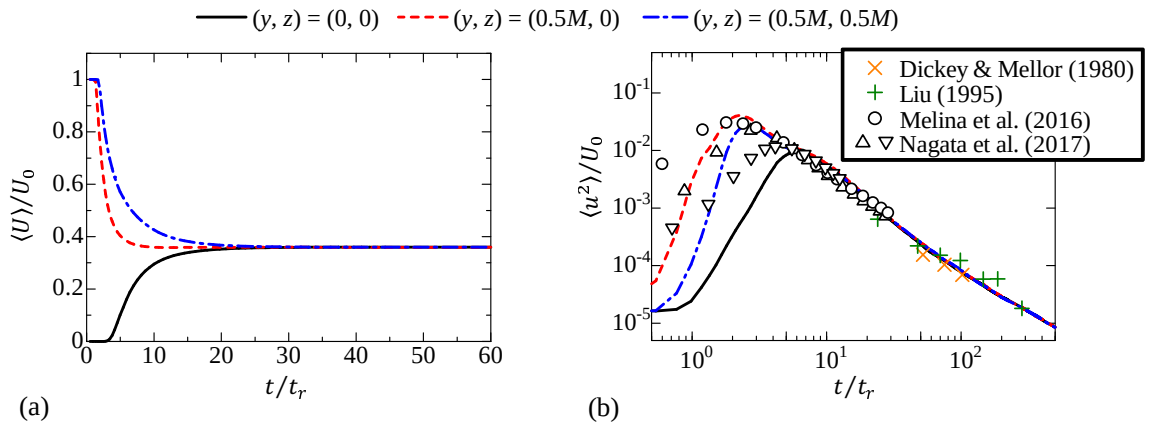

Figure 4. Temporal evolutions of (a) mean velocity $\langle U \rangle$ and (b) streamwise velocity variance $\langle u^2 \rangle$ at three y-z locations at $Re_M = 20,000$.

neutral and stratified fluids. *Journal of Fluid Mechanics* **99**, 13–31.

Hearst, J. & Lavoie, P. 2016 Effects of multi-scale and regular grid geometries on decaying turbulence. *Journal of Fluid Mechanics* **803**, 528–555.

Kitamura, T., Nagata, K., Sakai, Y., Sasoh, A., Terashima, O., Saito, H. & Harasaki, T. 2014 On invariants in grid turbulence at moderate Reynolds numbers. *Journal of Fluid Mechanics* **738**, 378–406.

Kozul, M., Chung, D. & Monty, J. P. 2016 Direct numerical simulation of the incompressible temporally developing turbulent boundary layer. *Journal of Fluid Mechanics* **796**, 437–472.

Krogstad, P.-Å. & Davidson, P. A. 2010 Is grid turbulence Saffman turbulence? *Journal of Fluid Mechanics* **642**, 373–394.

Liu, H.-T. 1995 Energetics of grid turbulence in a stably stratified fluid. *Journal of Fluid Mechanics* **296**, 127–157.

Melina, G., Bruce, P. J. K. & Vassilicos, J. C. 2016 Vortex shedding effects in grid-generated turbulence. *Physical Review Fluids* **1**, 044402.

Nagata, K., Saiki, T., Sakai, Y., Ito, Y. & Iwano, K. 2017 Effects of grid geometry on non-equilibrium dissipation in grid turbulence. *Physics of Fluids* **29**, 015102.

Simmons, L. F. G. & Salter, C. 1934 Experimental investigation and analysis of the velocity variations in turbulent flow. *Proceedings of the Royal Society A* **145**, 212–234.

Sinhuber, M., Bodenschatz, E. & Bewley, G. P. 2015 Decay of turbulence at high Reynolds numbers. *Physical Review Letters* **114**, 034501.

Watanabe, T., Zhang, X. & Nagata, K. 2018 Turbulent/non-turbulent interfaces detected in DNS of incompressible turbulent boundary layers. *Physics of Fluids* **30**, 035102.